THE JOURNAL OF PHYSICAL CHEMISTRY C
A JOURNAL OF THE AMERICAN CHEMICAL SOCIETY

pubs.acs.org/JPCC

Article

Interfacial Vibrational Spectroscopy of the Water Bending Mode on Ice I_h

Prerna Sudera, Jenée D. Cyran, Mischa Bonn,* and Ellen H. G. Backus*

Cite This: *J. Phys. Chem. C* 2021, 125, 22937−22942

Read Online

ACCESS | Metrics & More | Article Recommendations | Supporting Information

ABSTRACT: We study the molecular-level properties of the single-crystal ice I_h surface using interface-specific sum frequency generation spectroscopy. We probe the water vibrational bend region around 1650 cm^{-1} of the basal plane of hexagonal ice to understand the interfacial structure from vibrational properties. As opposed to the stretch mode of ice, the bending mode response depends very weakly on temperature. The large line width of the bending mode response, relative to the response on water, is inconsistent with inhomogeneous broadening and points to ultrafast pure dephasing. The bending mode of ice provides an excellent means to study adsorbate−ice interactions and understand differences in ice and water reactivity.

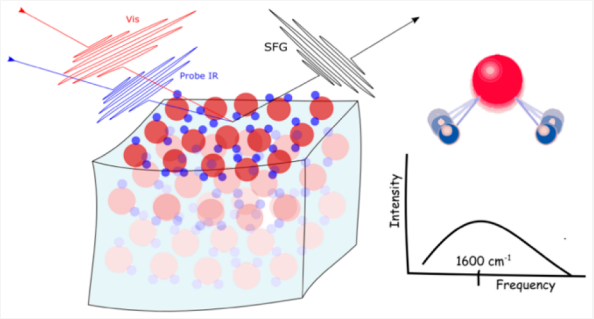

INTRODUCTION

The water−air and ice−air interfaces act as active sites for chemical reactions in both natural and engineering settings. Water molecules at the surface truncate the hydrogen bond network, which leads to unique physical properties that deviate from the bulk. The properties of interfacial water molecules have been extensively studied owing to their relevance in atmospheric,[1,2] biological,[3] electrochemical,[4,5] and geological sciences.[6] Ice interfaces have raised particular scientific interest owing to their reported high catalytic activity[7,8] and implications in frost heave, supraglacial chemistry,[9] and exchange of trace gases establishing atmospheric concentrations of species.[10] Information on the molecular properties of specifically the interface can be obtained with surface-specific vibrational spectroscopic methods, such as sum frequency generation (SFG) spectroscopy.[11,12] As a second-order nonlinear technique, SFG is inherently interface-specific owing to its selection rule that inversion symmetry must be broken for the signal to be generated. In this method, two laser beams, an infrared beam in resonance with a vibrational transition, and a visible beam for upconversion are overlapped in space and time. An SFG signal is generated at the sum of the frequencies of the two incoming laser beams. When the infrared beam is vibrationally resonant with surface molecules, the signal is enhanced. The SFG intensity as a function of infrared frequency thus provides the vibrational spectrum of specifically the interfacial molecules.

SFG research has traditionally focused on the ∼3300 cm^{-1} OH stretch mode of water in the study of interfacial properties of aqueous systems. The stretch mode frequency is correlated to hydrogen bond strength,[13,14] allowing access to the molecular structure information from spectroscopic observables. The stretch mode region of water gives a relatively high intensity compared to other vibrational modes, simplifying signal detection.

Despite the clear advantages, water vibrational stretch mode spectra can be challenging to interpret because of the strong effects of inter- and intramolecular couplings on the spectral line shape.[15−18] This coupling causes delocalization of vibrational OH stretch quanta, affecting the vibrational response. Further complications appear in the presence of other moieties with OH groups because of interference of the vibrational OH stretch of water with that of alcohols, other biomolecules, etc. The HOH bending mode of water can act as an insightful alternative to the stretch mode as it avoids such complications. The weaker intermolecular coupling for the bending mode and the correlation of the bending mode frequency to the hydrogen-bonding strength can complement the stretch mode results.[19,20] Because of its smaller transition dipole moment, the bending mode is expected to be less influenced by intermolecular dipole−dipole coupling, which was recently experimentally verified for water interfaces.[21] Furthermore, the bending mode of water is spectrally separate from the C−O−H and C−N−H bending modes of alcohols and biomolecules, making such composite systems simpler to study. The vibrational bending region has thus recently gained interest for obtaining molecular information on both bulk and interfacial systems.

Received: September 12, 2021
Revised: September 22, 2021
Published: October 12, 2021

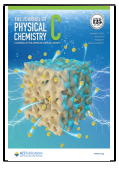

https://doi.org/10.1021/acs.jpcc.1c08046
J. Phys. Chem. C 2021, 125, 22937−22942

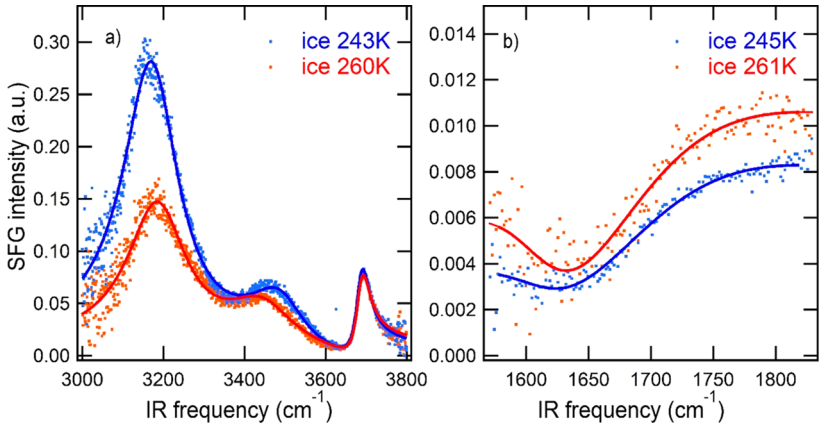

Figure 1. Experimental SFG measurements (dots) and fits (solid lines) in the vibrational stretch (a) and (b) bending mode region recorded from the surface of ice at two different temperatures, both measured using SSP polarization combination. The intensity axes in the left and right panels can be directly compared, indicating that the bending mode intensity is at least an order of magnitude smaller than that of the stretch mode.

The first SFG measurements of the vibrational bending mode of interfacial water, at ∼1650 cm^{-1}, dates back to 2012,[22] but has not yet been reported for ice. Previous theoretical work has shown that, for ice, the total dipole moment is reduced because of anticorrelated effects of permanent and induced dipole moments, indicating it is more challenging to determine the bending mode response from the surface of ice than of water.[23,24] Nevertheless, the bending mode region of interfacial ice is of fundamental importance, as its line shape may provide information on the low-frequency excitations and bending−libration coupling mechanisms[25] at interfaces, and on the bending overtone, which determines the rate of vibrational energy relaxation.[26] As the bending mode is expected to be a more "local" probe than the stretch mode, it can be important for studies of adsorbate-based systems on the surface of ice, allowing one to observe spectral changes without intermolecular coupling effects.[23]

METHODS

Ice Sample Preparation. Single-crystalline ice boules with a diameter of ∼6 cm were grown using the Czochralski method.[27] After confirmation of single crystallinity under a cross-polarizer setup, a thin slice of ice was cut from the boule to analyze the orientation of the ice crystal using the etch-pit technique.[28] Subsequently, from the boule, an ∼5 mm slice with the basal plane orientation was obtained using a band saw and formed into a 44 mm diameter sample using a heated metal mold. The sample was mounted onto a microtome and cut to optically flat gradeness using a triple-faceted blade from Leica. The sample was subsequently enclosed in a cell with a CaF_2 window and annealed for ∼12−15 h before a measurement. In the setup, the ice cell was rotating on a cooling copper stage during the entire measurement to avoid accumulated heat effects from the laser beams.

SFG and FTIR Setups. A femtosecond Ti-Saphhire amplified laser system (Coherent Libra) provided 800 nm, ∼50 fs pulses at a repetition rate of 1 kHz, with an output power of 5 W. A part of the visible output (∼2 W) was used to pump an optical parametric amplifier (TOPAS light conversion), generating broad band IR pulses covering the bending mode region. Another part (∼1 W) of the visible beam went through an etalon to generate a narrow pulse of approximately 20 cm^{-1} bandwidth. To generate the SFG signal, the visible and IR pulses were overlapped spatially and temporally on the sample at incident angles of 64° and 40°, respectively, with respect to the surface normal. At the sample, the visible and IR pulse energies were roughly 10 and 1 μJ, respectively. The SFG signal was focused onto an electron-multiplied CCD (EMCCD) camera (Andor) and dispersed by a spectrometer (Acton). The spectra were taken in two polarization combinations: SSP and PPP where the polarization combination stands in the order of the polarizations of the SFG, visible, and IR light. The SFG measurements were conducted for 20 min on ice and 4 min on water, typically 10−15 times. The averaged sample spectrum was background-subtracted and then normalized using a reference z-cut quartz spectrum measured in SSP polarization. Data in the stretch mode were collected on a different setup, the details of which are mentioned in the Supporting Information of our previous work.[29]

The ice sample for the infrared measurements is prepared by pressing a water droplet between two windows and placed in a cryostat. The infrared spectra are measured using a PerkinElmer 881 double-beam IR spectrometer.

RESULTS AND DISCUSSION

Here, we report vibrational bending mode spectra of interfacial ice I_h, measured using SFG spectroscopy (see Supporting Information for experimental details). The single-crystalline ice samples are oriented to measure the basal plane. The different planes of ice, basal, and prism faces expose different termination motifs and, thus, could alter the SFG response. Figure 1a,b shows SFG spectra of ice in the vibrational stretch and bending mode regions, respectively, at comparable temperatures in the SSP polarization combination. The stretch mode spectrum is dominated by a signal at roughly 3200 cm^{-1} assigned to O−H modes hydrogen-bonded to neighbors. The signal at 3700 cm^{-1} originates from so-called free OH groups, whereas the 3500 cm^{-1} could be mainly attributed to the asymmetric stretch mode of fully coordinated water molecules.[30] As apparent from Figure 1a, the ice surface exhibits a strong temperature dependence in the OH stretch region, with an ∼100% intensity increase for an ∼7% temperature decrease from 260 to 243 K. A possible explanation for this signal increase could be the enhanced orientation of interfacial water molecules at lower temperatures. However, MD simulations, shown in Figure S6, reveal that the orientational ordering of water molecules in the top two bilayers on the ice surface can

https://doi.org/10.1021/acs.jpcc.1c08046
J. Phys. Chem. C 2021, 125, 22937−22942

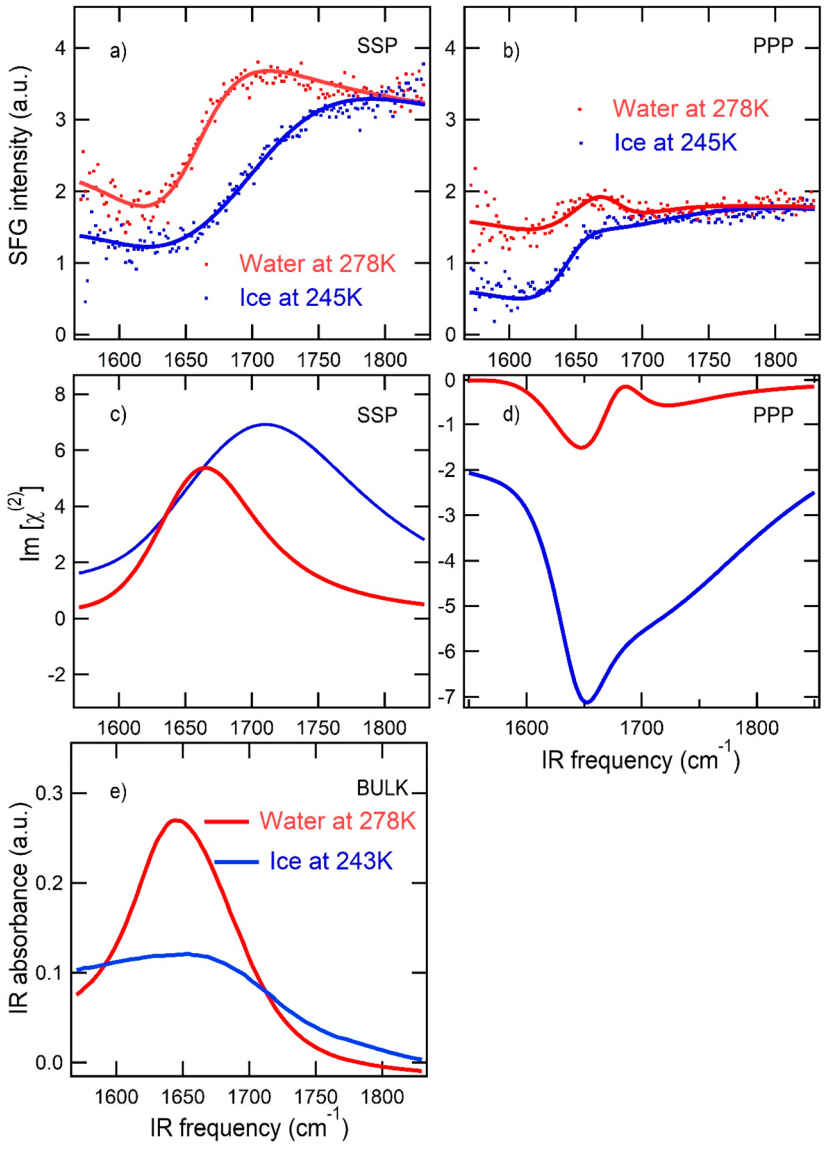

Figure 2. (a, b) Experimental SFG measurements (dots) and fits (solid lines) in the vibrational bending mode region of interfacial ice (blue) and water (red) with SSP measurements depicted in the left column and PPP in the right. Water and ice spectra, also SSP and PPP, are plotted on the same scale; see the Supporting Information for correction due to intensity alteration on the window of the ice cell. (c, d) Imaginary $\chi^{(2)}$ for both polarization combinations obtained from the spectral fits. (e) Linear infrared absorption spectra for bulk ice and water in the H−O−H bending region.

account only for an ∼10% increase in the SFG intensity over this limited temperature interval. Therefore, only a small fraction of the signal increase can be explained by enhanced orientation. Thus, the major change in the stretch mode intensity for interfacial ice is attributed to temperature-dependent intermolecular coupling in the stretch region.[31] In contrast, Figure 1b shows no indication of a similar intensity increase for the interfacial ice bending mode region upon lowering the temperature, in-line with the notion that bending modes are weakly coupled. The response in the bending region is, however, less straightforward than that in the stretch region. For the stretch region, several clear peaks can be identified. In contrast, the bending mode response appears derivative-like because of a relatively sizable nonresonant contribution to the overall signal, as apparent from the high baseline relative to the signal size.

Figure 1a reveals a red shift of the stretch mode upon a decrease in temperature, as reported before.[32] A red shift in the stretch mode region is associated with stronger hydrogen bonding. Conversely, stronger hydrogen bonding is reflected by a blue shift of the bending mode frequency, as first shown by Falk.[33] For the given temperature interval, the ∼15 cm^{-1} red shift of the low-frequency peak of ice in the stretch region translates to a negligible frequency shift in the bending region, as per the empirically inferred relationship[34] between the frequencies of the two modes. Indeed, no shift is apparent from the data in Figure 1b. Having established that the bending mode is less affected by intermolecular coupling, we further analyze the bending mode response at the ice interface and compare it with the response of water.

Figure 2a,b represents the bending mode SFG intensity obtained from the interfaces of ice and water for the polarization combinations SSP (left column) and PPP (right

https://doi.org/10.1021/acs.jpcc.1c08046
J. Phys. Chem. C 2021, 125, 22937−22942

column) as a function of the IR frequency. From the raw data, it is apparent that the bending mode response of ice is blue-shifted and substantially broadened compared to that of water. Both effects are qualitatively also present in the bulk infrared response (Figure 2e), but the blue shift is more pronounced at the interface. Perhaps remarkably, the SFG intensity for ice and water in the bending mode region is comparable. This observation is remarkable for two reasons: First of all, the intensities in the stretch mode region are strikingly different, with interfacial ice having a considerably higher intensity than water, as shown in the Supporting Information. This difference is in-line with the strong intermolecular coupling present in the stretch region for ice[31] and its absence in the bending region. Second, the bulk infrared response of the ice bending mode is substantially weaker (by a factor 2−3) than that of liquid water (see Figure 2e). Nonetheless, the SFG bending mode intensities are very similar for ice and water.

The bend spectra display dispersive line shapes for both polarization combinations. The PPP spectra are less intense for both ice and water, compared to the SSP spectra. The SSP response is most insightful because it is determined by one independent ($\chi^{(2)}_{xxz} = \chi^{(2)}_{yyz}$) element of the $\chi^{(2)}$ second rank tensor; the PPP response, in contrast, contains contributions from two ($\chi^{(2)}_{xxz}$ and $\chi^{(2)}_{zzz}$) independent tensor elements,[35] as explained in the Supporting Information. To quantify the observed spectral changes, the SSP spectra are fitted using a purely real nonresonant contribution and two complex resonant Lorentzian contributions (see Supporting Information for fit functions and Table 1 for the fitting parameters).

Table 1. Fitting Parameters for the Bending Mode Spectra of SSP and PPP Polarization Combinations for Both Ice and Water[a]

	ice SSP	water SSP	ice PPP	water PPP
NR Amp	−0.14	−0.16	0.1	0.13
ω_1 cm^{-1}	1612	1612	1612	1612
$2\sigma(\omega_1)$ cm^{-1}	130	130	130	130
A (ω_1)	0.9 (2.57)	1.3	−0.54 (−1.5)	−0.78
ω_2 cm^{-1}	1706 (1689)	1661	1706 (1689)	1661
$2\sigma(\omega_2)$ cm^{-1}	200 (300)	110	200 (300)	110
A (ω_2)	−7.3 (−13.8)	−3.6	4.38 (8.28)	2.16
ω_3 cm^{-1}			1646	1679
$2\sigma(\omega_3)$ cm^{-1}			60	60
A (ω_3)			1.1	−0.8

[a]Values in brackets for ice denote alternative fitting parameters.

The interfacial water SSP spectrum was described in accordance with previously reported parameters,[20] in agreement with the reported heterodyne measurements of the water−air interface.[36] The high-frequency resonance is attributed to a DD-type water molecule, which donates two hydrogen bonds. The low-frequency resonance corresponds to a D-type molecule having one H-bond donating OH group and a dangling, free OH group.[19,20,37,38] Thus, the low- and high-frequency contributions correspond to water molecules having a free OH and the strongly hydrogen-bonded water molecules at the surface, respectively.

To fit the interfacial ice SSP spectrum, the center frequency and line width of the low-frequency feature, corresponding to interfacial molecules with a free OH, are kept similar to the fit for water. This assumption is based on the observation that the free OH groups at the interface of water and ice have a very similar stretch frequency (Figure S5). The amplitude, central frequency, and line width of the high-frequency bend feature are allowed to vary between ice and water spectra. From fitting of the interfacial ice SSP spectrum, a strong correlation between the position and width of the high-frequency peak was observed. The peak frequency varied between 1706 and 1689 cm^{-1} when the peak width is varied between 200 and 300 cm^{-1}; Table 1 shows the fitting parameters, and Figure 2c shows the imaginary part of the fitted response function.

A comparison of the interfacial ice and water spectra of the SSP polarization combination reveals that the ice bending mode is blue-shifted by ∼35 cm^{-1} (taking an average peak position of 1697 cm^{-1} for the ice SSP response). This blue shift for the bending mode feature represents stronger hydrogen bonding. From the empirical relationship[34] between the bend and stretch frequencies, a blue shift of 35 cm^{-1} for the bending mode of ice corresponds very well with the ∼200 cm^{-1} red shift observed (see Supporting Information) for the stretch mode in ice compared to that in water.

The vibrational bend bandwidth is roughly doubled for interfacial ice (200−300 cm^{-1}) compared to water (110 cm^{-1}), as is apparent from the raw data in Figure 2a and the fits presented in Figure 2c and Table 1. This is in strong contrast to the OH stretch line shape being much narrower for interfacial ice than for interfacial water (Supporting Information), further narrowing upon lowering of the temperature of ice.[39] If the ice surface bending mode was inhomogeneously broadened, the observed bandwidth, >200 cm^{-1}, would translate to an extremely broad band of more than 1000 cm^{-1} in the stretch region, using the empirical relationship mentioned above. This is clearly not observed, indicating that the bending mode of ice is predominantly homogeneously broadened, with a short dephasing time of the ice bending mode, which would include the pure dephasing time, population, and orientational relaxation. Ultrafast studies of the bulk water bending mode report a vibrational lifetime of ∼170 fs[21,40] and an ultrafast anisotropy decay of 80 fs.[41] The >200 cm^{-1} bandwidth of the bending mode of ice compared to that of water, and the incompatibility with the inhomogeneous broadening mechanism, suggests sub-25 fs vibrational dephasing times for the bending mode of ice. Consistent with the interfacial spectra, the bulk bending mode spectrum also has a broader line shape for ice, as seen from Figure 2e, also opposite to the stretch mode.[42]

The fitting for the PPP spectra was conducted by keeping the SSP parameters corresponding to the effective (i.e., including the Fresnel factors) $\chi^{(2)}_{xxz}$ consistent (the amplitudes were adjusted according to prefactors as per eq 1 in the Supporting Information) and by adding an additional peak representing an effective $\chi^{(2)}_{zzz}$ as the additional tensor element in PPP spectra. The nonresonant signal contribution is kept purely real. Both PPP spectra can be very well fitted (see Figure 2b) and result in an additional peak at 1646 and 1679 cm^{-1} for ice and water, respectively.

From a comparison of the raw data for the two polarization combinations, we observe a spectral shift to the red side for the PPP spectrum compared to that for the SSP spectrum for both ice and water (Figure S3). Considering the complications of a direct comparison from the data fits according to the tensor elements described before, the spectral shift was quantified using simple sigmoidal fits (more details can be found in the Supporting Information) to the ice and water spectra. For water, the PPP spectrum shift is quantified to be ∼20 cm^{-1} to

https://doi.org/10.1021/acs.jpcc.1c08046
J. Phys. Chem. C 2021, 125, 22937−22942

the red side. This shift is in-line with the 15 cm^{-1} shift reported before,[38] explained by the authors as an interference effect of two types of hydrogen-bonding populations giving the same resonances in both the PPP and SSP responses. However, we observe that an additional peak is needed to describe the PPP response; solely, the SSP response is not enough. Interestingly, we observe an even larger frequency red shift for PPP compared to that for SSP in the case of interfacial ice, amounting to ~50 cm^{-1} as per the sigmoidal fit. This 50 cm^{-1} shift is in good agreement with the frequency difference between ω_2 and ω_3 in Table 1, indicating that for ice the PPP signal is dominated by the $\chi^{(2)}_{zzz}$ tensor element. See the Supporting Information for an elaborate discussion on the Fresnel factors showing that optical effects due to setup geometry are not causing the differences.

CONCLUSIONS

In conclusion, this work has shed light upon the observed contrasting features of the bending mode spectra for ice and water compared to the stretch mode. Stronger hydrogen bonding for ice manifests as a red shift in the stretch mode region and a blue shift in the bending mode region, as was empirically predicted and experimentally confirmed by our measurements. A comparable intensity of the bending mode for ice and water (unlike for the stretch mode), and little or no temperature dependence in our range of temperature variation, points toward negligible intermolecular coupling for the bending mode region. The anomalously increased bandwidth of ice in the bending mode compared to that of water points toward the line-broadening mechanism to be predominantly homogeneous, unlike that in the stretch mode. Also, polarization-dependent studies in the bending mode region indicate an inherent 20 and 50 cm^{-1} frequency shift between the SSP and PPP spectra for ice and water, respectively, the origins of which remain incompletely understood. These results, providing insights into the bending mode region of ice, also provide the basis for exploring a plethora of molecules, in particular, ice-binding proteins or small organic molecules with carbonyl groups, on the surface of ice.

ASSOCIATED CONTENT

Supporting Information

The Supporting Information is available free of charge at https://pubs.acs.org/doi/10.1021/acs.jpcc.1c08046.

Details on fitting, description of the influence of Fresnel Factors and the CaF_2 window, temperature-dependent results of the OH stretch region, and discussion on SFG intensity changes due to change of orientation of water molecules (PDF)

AUTHOR INFORMATION

Corresponding Authors

Ellen H. G. Backus − *Department for Molecular Spectroscopy, Max Planck Institute for Polymer Research, 55128 Mainz, Germany; Department of Physical Chemistry, University of Vienna, 1090 Vienna, Austria;* orcid.org/0000-0002-6202-0280; Email: ellen.backus@univie.ac.at

Mischa Bonn − *Department for Molecular Spectroscopy, Max Planck Institute for Polymer Research, 55128 Mainz, Germany;* orcid.org/0000-0001-6851-8453; Email: bonn@mpip-mainz.mpg.de

Authors

Prerna Sudera − *Department for Molecular Spectroscopy, Max Planck Institute for Polymer Research, 55128 Mainz, Germany*

Jenée D. Cyran − *Department for Molecular Spectroscopy, Max Planck Institute for Polymer Research, 55128 Mainz, Germany; Department of Chemistry and Biochemistry, Baylor University, Waco, Texas 76706, United States;* orcid.org/0000-0002-5278-9854

Complete contact information is available at: https://pubs.acs.org/10.1021/acs.jpcc.1c08046

Funding

Open access funded by Max Planck Society.

Notes

The authors declare no competing financial interest.

The data that support the findings of this study are available from the corresponding authors upon request.

ACKNOWLEDGMENTS

We thank Yuki Nagata and Takakazu Seki for their very fruitful ideas and helpful discussions, Walter Scholdei for performing the bulk IR experiments, and Marc-Jan van Zadel for his excellent technical support.

REFERENCES

(1) Herrmann, H. Kinetics of Aqueous Phase Reactions Relevant for Atmospheric Chemistry. *Chem. Rev.* **2003**, *103* (12), 4691−4716.

(2) Aloisio, S.; Francisco, J. S. Radical-Water Complexes in Earth's Atmosphere. *Acc. Chem. Res.* **2000**, *33* (12), 825−830.

(3) Scatena, L. F. Water at Hydrophobic Surfaces: Weak Hydrogen Bonding and Strong Orientation Effects. *Science (Washington, DC, U. S.)* **2001**, *292* (5518), 908−912.

(4) Park, S.; Shao, Y.; Liu, J.; Wang, Y. Oxygen Electrocatalysts for Water Electrolyzers and Reversible Fuel Cells: Status and Perspective. *Energy Environ. Sci.* **2012**, *5* (11), 9331.

(5) Toney, M. F.; Howard, J. N.; Richer, J.; Borges, G. L.; Gordon, J. G.; Melroy, O. R.; Wiesler, D. G.; Yee, D.; Sorensen, L. B. Voltage-Dependent Ordering of Water Molecules at an Electrode-Electrolyte Interface. *Nature* **1994**, *368* (6470), 444−446.

(6) Hydro | Earth https://earth.gsfc.nasa.gov/index.php/hydro (accessed 2021-05-31).

(7) Tolbert, M. A.; Rossi, M. J.; Golden, D. M. Antarctic Ozone Depletion Chemistry: Reactions of N2O5 with H2O and HCl on Ice Surfaces. *Science (Washington, DC, U. S.)* **1988**, *240* (4855), 1018−1021.

(8) Bartels-Rausch, T.; Jacobi, H.-W.; Kahan, T. F.; Thomas, J. L.; Thomson, E. S.; Abbatt, J. P. D.; Ammann, M.; Blackford, J. R.; Bluhm, H.; Boxe, C.; Domine, F.; Frey, M. M.; Gladich, I.; Guzmán, M. I.; Heger, D.; Huthwelker, T.; Klán, P.; Kuhs, W. F.; Kuo, M. H.; Maus, S.; Moussa, S. G.; McNeill, V. F.; Newberg, J. T.; Pettersson, J. B. C.; Roeselová, M.; Sodeau, J. R. A Review of Air-Ice Chemical and Physical Interactions (AICI): Liquids, Quasi-Liquids, and Solids in Snow. *Atmos. Chem. Phys.* **2014**, *14* (3), 1587−1633.

(9) Stibal, M.; Sabacká, M.; Zárský, J. Biological Processes on Glacier and Ice Sheet Surfaces. *Nat. Geosci.* **2012**, *5* (11), 771−774.

(10) Kahan, T. F.; Wren, S. N.; Donaldson, D. J. A Pinch of Salt Is All It Takes: Chemistry at the Frozen Water Surface. *Acc. Chem. Res.* **2014**, *47* (5), 1587−1594.

(11) Shen, Y. R. Surface Properties Probed by Second-Harmonic and Sum-Frequency Generation. *Nature* **1989**, *337* (6207), 519−525.

(12) Lambert, A. G.; Davies, P. B.; Neivandt, D. J. Implementing the Theory of Sum Frequency Generation Vibrational Spectroscopy: A Tutorial Review. *Appl. Spectrosc. Rev.* **2005**, *40* (2), 103−145.

(13) Ford, T. A.; Falk, M. Hydrogen Bonding in Water and Ice. *Can. J. Chem.* **1968**, *46* (22), 3579−3586.

(14) Rey, R.; Møller, K. B.; Hynes, J. T. Hydrogen Bond Dynamics in Water and Ultrafast Infrared Spectroscopy. *J. Phys. Chem. A* **2002**, *106* (50), 11993−11996.
(15) Schaefer, J.; Backus, E. H. G.; Nagata, Y.; Bonn, M. Both Inter- and Intramolecular Coupling of O-H Groups Determine the Vibrational Response of the Water/Air Interface. *J. Phys. Chem. Lett.* **2016**, *7* (22), 4591−4595.
(16) Buch, V. Molecular Structure and OH-Stretch Spectra of Liquid Water Surface. *J. Phys. Chem. B* **2005**, *109* (38), 17771−17774.
(17) Torii, H. Effects of Intermolecular Vibrational Coupling and Liquid Dynamics on the Polarized Raman and Two-Dimensional Infrared Spectral Profiles of Liquid *N*,*N*-Dimethylformamide Analyzed with a Time-Domain Computational Method. *J. Phys. Chem. A* **2006**, *110* (14), 4822−4832.
(18) Auer, B. M.; Skinner, J. L. IR and Raman Spectra of Liquid Water: Theory and Interpretation. *J. Chem. Phys.* **2008**, *128* (22), 224511.
(19) Ni, Y.; Skinner, J. L. IR and SFG Vibrational Spectroscopy of the Water Bend in the Bulk Liquid and at the Liquid-Vapor Interface, Respectively. *J. Chem. Phys.* **2015**, *143* (1), 014502.
(20) Seki, T.; Sun, S.; Zhong, K.; Yu, C. C.; MacHel, K.; Dreier, L. B.; Backus, E. H. G.; Bonn, M.; Nagata, Y. Unveiling Heterogeneity of Interfacial Water through the Water Bending Mode. *J. Phys. Chem. Lett.* **2019**, *10* (21), 6936−6941.
(21) Yu, C.-C.; Chiang, K.-Y.; Okuno, M.; Seki, T.; Ohto, T.; Yu, X.; Korepanov, V.; Hamaguchi, H.; Bonn, M.; Hunger, J.; Nagata, Y. Vibrational Couplings and Energy Transfer Pathways of Water's Bending Mode. *Nat. Commun.* **2020**, *11* (1), 5977.
(22) Vinaykin, M.; Benderskii, A. Vibrational Sum-Frequency Spectrum of the Water Bend at the Air/Water Interface. *J. Phys. Chem. Lett.* **2012**, *3*, 3348−3352.
(23) Hernandez, J.; Uras, N.; Devlin, J. P. Molecular Bending Mode Frequencies of the Surface and Interior of Crystalline Ice. *J. Chem. Phys.* **1998**, *108* (11), 4525−4529.
(24) Imoto, S.; Xantheas, S. S.; Saito, S. Molecular Origin of the Difference in the HOH Bend of the IR Spectra between Liquid Water and Ice. *J. Chem. Phys.* **2013**, *138* (5), 054506.
(25) Rey, R.; Ingrosso, F.; Elsaesser, T.; Hynes, J. T. Pathways for H 2 O Bend Vibrational Relaxation in Liquid Water. *J. Phys. Chem. A* **2009**, *113* (31), 8949−8962.
(26) van der Post, S. T.; Hsieh, C.-S.; Okuno, M.; Nagata, Y.; Bakker, H. J.; Bonn, M.; Hunger, J. Strong Frequency Dependence of Vibrational Relaxation in Bulk and Surface Water Reveals Sub-Picosecond Structural Heterogeneity. *Nat. Commun.* **2015**, *6* (1), 8384.
(27) Roos, D. v. d. S. Rapid Production of Single Crystals of Ice. *J. Glaciol.* **1975**, *14* (71), 325−328.
(28) Knight, C. A. Formation of Crystallographic Etch Pits on Ice, and Its Application to the Study of Hailstones. *J. Appl. Meteorol.* **1966**, *5* (5), 710−714.
(29) Sudera, P.; Cyran, J. D.; Deiseroth, M.; Backus, E. H. G.; Bonn, M. Interfacial Vibrational Dynamics of Ice Ih and Liquid Water. *J. Am. Chem. Soc.* **2020**, *142*, 12005.
(30) Smit, W. J.; Tang, F.; Nagata, Y.; Sánchez, M. A.; Hasegawa, T.; Backus, E. H. G.; Bonn, M.; Bakker, H. J. Observation and Identification of a New OH Stretch Vibrational Band at the Surface of Ice. *J. Phys. Chem. Lett.* **2017**, *8* (15), 3656−3660.
(31) Ishiyama, T.; Takahashi, H.; Morita, A. Origin of Vibrational Spectroscopic Response at Ice Surface. *J. Phys. Chem. Lett.* **2012**, *3* (20), 3001−3006.
(32) Wei, X.; Miranda, P. B.; Zhang, C.; Shen, Y. R. Sum-Frequency Spectroscopic Studies of Ice Interfaces. *Phys. Rev. B: Condens. Matter Mater. Phys.* **2002**, *66* (8), 085401.
(33) Falk, M. The Frequency of the HOH Bending Fundamental in Solids and Liquids. *Spectrochim. Acta Part A Mol. Spectrosc.* **1984**, *40* (1), 43−48.
(34) Seki, T.; Yu, C. C.; Yu, X.; Ohto, T.; Sun, S.; Meister, K.; Backus, E. H. G.; Bonn, M.; Nagata, Y. Decoding the Molecular Water Structure at Complex Interfaces through Surface-Specific Spectroscopy of the Water Bending Mode. *Phys. Chem. Chem. Phys.* **2020**, *22* (19), 10934−10940.
(35) Zhuang, X.; Miranda, P. B.; Kim, D.; Shen, Y. R. Mapping Molecular Orientation and Conformation at Interfaces by Surface Nonlinear Optics. *Phys. Rev. B: Condens. Matter Mater. Phys.* **1999**, *59* (19), 12632−12640.
(36) Ahmed, M.; Nihonyanagi, S.; Kundu, A.; Yamaguchi, S.; Tahara, T. Resolving the Controversy over Dipole versus Quadrupole Mechanism of Bend Vibration of Water in Vibrational Sum Frequency Generation Spectra. *J. Phys. Chem. Lett.* **2020**, *11* (21), 9123−9130.
(37) Moberg, D. R.; Straight, S. C.; Paesani, F. Temperature Dependence of the Air/Water Interface Revealed by Polarization Sensitive Sum-Frequency Generation Spectroscopy. *J. Phys. Chem. B* **2018**, *122* (15), 4356−4365.
(38) Dutta, C.; Benderskii, A. V. On the Assignment of the Vibrational Spectrum of the Water Bend at the Air/Water Interface. *J. Phys. Chem. Lett.* **2017**, *8* (4), 801−804.
(39) Wei, X.; Miranda, P. B.; Shen, Y. R. Surface Vibrational Spectroscopic Study of Surface Melting of Ice. *Phys. Rev. Lett.* **2001**, *86* (8), 1554−1557.
(40) Huse, N.; Ashihara, S.; Nibbering, E. T. J.; Elsaesser, T. Ultrafast Vibrational Relaxation of O-H Bending and Librational Excitations in Liquid H2O. *Chem. Phys. Lett.* **2005**, *404*, 389.
(41) Carpenter, W. B.; Fournier, J. A.; Biswas, R.; Voth, G. A.; Tokmakoff, A. Delocalization and Stretch-Bend Mixing of the HOH Bend in Liquid Water. *J. Chem. Phys.* **2017**, *147* (8), 084503.
(42) Riemenschneider, J.; Wulf, A.; Ludwig, R. The Effects of Temperature and H/D Isotopic Dilution on the Transmission and Attenuated Total Reflection FTIR Spectra of Water. *Z. Phys. Chem.* **2009**, *223* (9), 1011−1022.

https://doi.org/10.1021/acs.jpcc.1c08046
J. Phys. Chem. C 2021, 125, 22937−22942